European Journal of Medicinal Chemistry 250 (2023) 115160

Contents lists available at ScienceDirect

European Journal of Medicinal Chemistry

journal homepage: www.elsevier.com/locate/ejmech

Research paper

Amide containing NBTI antibacterials with reduced hERG inhibition, retained antimicrobial activity against gram-positive bacteria and *in vivo* efficacy

Maja Kokot [a,b], Matjaž Weiss [b], Irena Zdovc [c], Lidija Senerovic [d], Natasa Radakovic [d], Marko Anderluh [b], Nikola Minovski [a,**], Martina Hrast [b,*]

[a] Theory Department, Laboratory for Cheminformatics, National Institute of Chemistry, Hajdrihova 19, 1001, Ljubljana, Slovenia
[b] Department of Pharmaceutical Chemistry, Faculty of Pharmacy, University of Ljubljana, Aškerčeva Cesta 7, 1000, Ljubljana, Slovenia
[c] Institute of Microbiology and Parasitology, Veterinary Faculty, University of Ljubljana, Gerbičeva 60, 1000, Ljubljana, Slovenia
[d] Laboratory for Microbial Molecular Genetics and Ecology, Institute of Molecular Genetics and Genetic Engineering, University of Belgrade, Vojvode Stepe 444a, 11 042, Belgrade, Serbia

ARTICLE INFO

Keywords:
NBTIs
DNA gyrase
Topoisomerase IV
Antibacterials
MRSA
hERG inhibition
In vivo efficacy

ABSTRACT

Novel bacterial topoisomerase inhibitors (NBTIs) are new promising antimicrobials for the treatment of multidrug-resistant bacterial infections. In recent years, many new NBTIs have been discovered, however most of them struggle with the same issue - the balance between antibacterial activity and hERG-related toxicity. We started a new campaign by optimizing the previous series of NBTIs, followed by the design and synthesis of a new, amide-containing focused NBTI library to reduce hERG inhibition and maintain antibacterial activity against Gram-positive bacteria, including methicillin-resistant *Staphylococcus aureus* (MRSA). This optimization strategy yielded the lead compound **12** that exhibits potent antibacterial activity against Gram-positive bacteria, reduced hERG inhibition, no cardiotoxicity in zebrafish model, and a favorable *in vivo* efficacy in a neutropenic murine thigh infection model of MRSA infection.

1. Introduction

The continued development and spread of multidrug-resistant bacteria such as methicillin-resistant *Staphylococcus aureus* (MRSA) presents a significant threat to human health [1]. According to the U.S. Centers for Disease Control and Prevention (CDC), MRSA is a leading cause of complications and death in patients who get the flu and it is responsible for more than 10,000 deaths per year [2]. Still, new therapeutic alternatives for treating MRSA infections are urgently needed, given its role in both healthcare and the community [3].

Fluoroquinolones are one of the most commonly used antimicrobial agents that target bacterial type II topoisomerases, namely DNA gyrase and topoisomerase IV (topoIV) [4]. Acquired resistance in bacteria due to extensive use of fluoroquinolones has resulted in a dramatic decrease in their therapeutic usefulness [5], although some of the traditional ones are still used in the clinical practice (e.g., ciprofloxacin, moxifloxacin, and levofloxacin) [6]. Delafloxacin, a representative of the newer generation of fluoroquinolones is currently used for the treatment of acute bacterial skin infections [7]. This is due to the chemically different structure of delafloxacin compared to current fluoroquinolones that enhances its antibacterial activity in acidic environments, such as those found in *Staphylococcus aureus* infections [8,9]. Other non-ATPase, non-quinolone bacterial topoisomerases II inhibitors are quinolinepyrimidinetriones or spiropyrimidinetriones. They evolved from the lead compound QPT-1 (PNU-286607) [10,11] and the representative of this class - zoliflodacin (ETX0914) is currently in Phase III clinical trials for the treatment of *Neisseria gonorrhoeae* infections. Despite that zoliflodacin, like fluoroquinolones, inhibits supercoiling (DNA gyrase) and decatenation (topoIV) and stabilize the enzyme-DNA cleaved complex, religation of the cleaved DNA doesn't occur in the presence of

Abbreviations: NBTI, novel bacterial topoisomerase inhibitors; hERG, human ether-à-go-go-related gene; MRSA, methicillin-resistant *Staphylococcus aureus*; topoIV, topoisomerase IV; LHS, left-hand side; RHS, right-hand side; PAE, post-antibiotic effect.

* Corresponding author.
** Corresponding author.
E-mail addresses: nikola.minovski@ki.si (N. Minovski), martina.hrast@ffa.uni-lj.si (M. Hrast).

https://doi.org/10.1016/j.ejmech.2023.115160
Received 7 November 2022; Received in revised form 23 January 2023; Accepted 24 January 2023
Available online 2 February 2023

zoliflodacin as by fluoroquinolones. Consequently, no target-based cross-resistance with the quinolone class is observed [12]. A promising class of antibacterial agents named as "novel bacterial topoisomerase inhibitors" (NBTIs) was introduced about two decades ago [13–16]. Relative to fluoroquinolones and other non-quinolone antimicrobials, their peculiar chemical structure, the alternative binding site in bacterial topoisomerases as well as their substantially distinct mechanism of inhibition made them highly interesting and promising as future antibacterials in combating resistant bacteria [15,17–19]. The most advanced NBTI gepotidacin (GSK2140944) is currently in the third phase of clinical trials for the treatment of uncomplicated urogenital gonorrhea caused by *N. gonorrhoeae* [20,21] as well as uncomplicated urinary tract infections (acute cystitis) most commonly caused by *Escherichia coli* [22].

One of the important reasons for the limited number of NBTIs reaching clinical trials is their class-related inhibition of the human Ether-à-go-go-Related Gene (hERG) potassium channels in the heart [23], leading to a prolonged QT interval and subsequently life-threatening arrhythmias [24,25]. The guidelines toward reducing hERG inhibition are rather general and mostly encompass tuning of both structural and physicochemical features, such as removal of tertiary amine, structural modifications for reducing lipophilicity, and removal of oxygen-hydrogen bond acceptors [26].

It should be stressed, however that the majority of NBTIs comprise a secondary and/or tertiary amine in their structure as a part of the central linker moiety (Fig. 1, red). The analysis of the available crystal structures of *S. aureus* DNA gyrase-DNA-NBTI ternary complexes reveal that this secondary amine is critical for high affinity and consequently potent enzyme inhibition and antibacterial activity of NBTIs as it establishes an important salt bridge interaction with the Asp83 residue(s) of *S. aureus* GyrA subunits [15,17,18,27]. The same is also evident in our previously reported series of aminopiperidine-naphthyridine linked NBTIs where

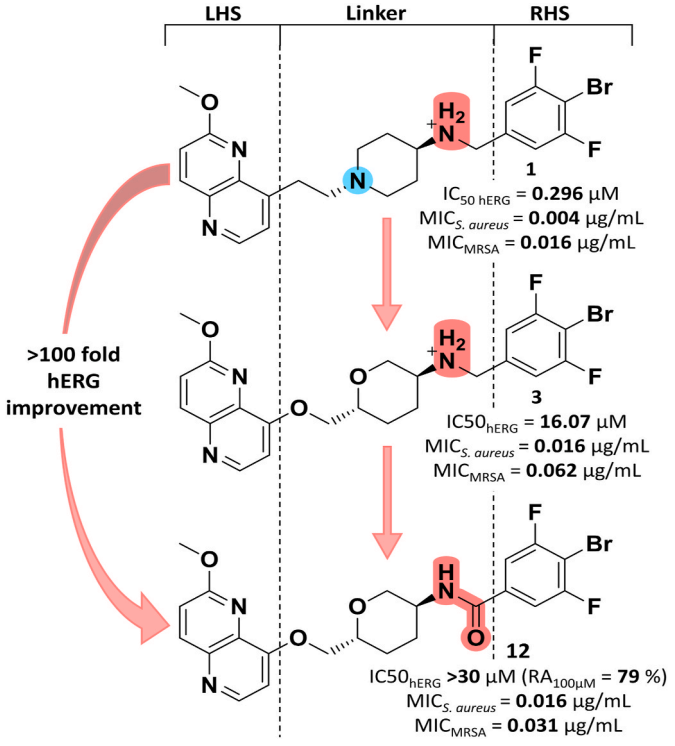

Fig. 1. Optimization process of amide containing series of NBTIs. Structural optimization strategy for reduced hERG inhibition and retained antibacterial activities and enzyme inhibition potencies of NBTIs, from 1 to 3 to 12. The general composition of NBTIs is above their structural formulae (LHS, linker, RHS).

the linker's secondary amine is indeed a key structural feature governing their antibacterial potency, however the linker's tertiary amine (Fig. 1, blue) undoubtedly and significantly contributes to hERG inhibition [28].

In the present work we considered the observation that substitution of the linker's secondary amine in the structure with an amide can contribute towards reducing hERG inhibition as previously reported by Lu et al. [29,30] and others [13,31]. Thus synthesized amide containing NBTI analogs exhibit lower hERG inhibition, while retaining their antibacterial activity thereby yielding a balanced activity-toxicity profile. Unfortunately, the efforts of Lu et al. to reduce hERG inhibition ended up with a series of NBTIs with rather substantial drop in the antibacterial activity [29]. In this work, we have overcome this issue and we present here a focused series of NBTIs comprising an amide linker that exhibit balanced activity-toxicity profile. Moreover, we also demonstrate the *in vivo* efficacy in a neutropenic murine thigh infection model of MRSA infection of three NBTI representatives with most balanced hERG IC_{50}/MIC ratio.

2. Results and discussion

2.1. NBTIs optimization strategy

Our recently reported crystal structure (PDB ID: 6Z1A) [17] revealed that halogen atom at the *para*-position of the phenyl right-hand side (RHS) moiety (Fig. 1) establishes strong symmetrical bifurcated halogen-bonding interactions with the backbone carbonyl oxygens of GyrA Ala68 residues in *S. aureus* DNA gyrase. By introducing electron-withdrawing groups at the *meta*-positions of the *p*-halogenated phenyl RHSs (i.e., *ortho*-relative to the halogen substituent) we notably enhanced the enzyme inhibitory and antibacterial activity of this series of NBTIs by intensifying their halogen-bonding strengths [32]. To reduce their hERG inhibitory activity, we initially synthesized an optimized small series of NBTI analogs by replacing the piperidine linker bearing the unwanted tertiary amine with a cyclohexane or tetrahydropyran and replacing the linker's ethylene bridge with oxymethylene or 1-hydroxyethylene [28]. These structural alterations led us to excellent enzyme inhibitory and antibacterial activity, and diminished hERG inhibition that still needed optimization to reach desired safety for *in vivo* studies. To further reduce the hERG inhibitory activity, a new focused library of NBTIs was designed substantiated on replacing the secondary amine with an amide, thus completely avoiding basic functionality within the linker moiety (Fig. 1).

2.2. Chemistry

The synthesis of new NBTIs is presented on Scheme 1. As demonstrated, the synthetic procedure consists of two steps: first a 1,1′-carbonyldiimidazole (CDI) was used to activate *p*-halogenated benzoic acids (**A1**, **A2**, and **A3**) into an intermediate, which in the next step reacted with amines containing various linker moieties (**B1**, **B2**, and **B3**) to yield the final amide containing compounds (**5**–**13**). **B1**, **B2**, and **B3** were synthesized by the procedure described in our previous publication [28]. Synthesis details are given in the Experimental section.

2.3. Biological evaluation and structure-activity relationship

The focused library of optimized NBTIs and their inhibitory potencies on bacterial type II topoisomerase enzymes are presented in Table 1, while their antibacterial activities are summarized in Table 2 and Table S2. The replacement of methyleneamine with an amide in general resulted in decrease of the inhibitory potency for all of the enzymes as well as decrease in the antibacterial activity. The amide containing compounds with piperidine (**6**) and tetrahydropyran (**12**) linkers had slightly weaker enzyme inhibitory potencies compared to those containing secondary amine (**1** and **3**) with tetrahydropyran comprising

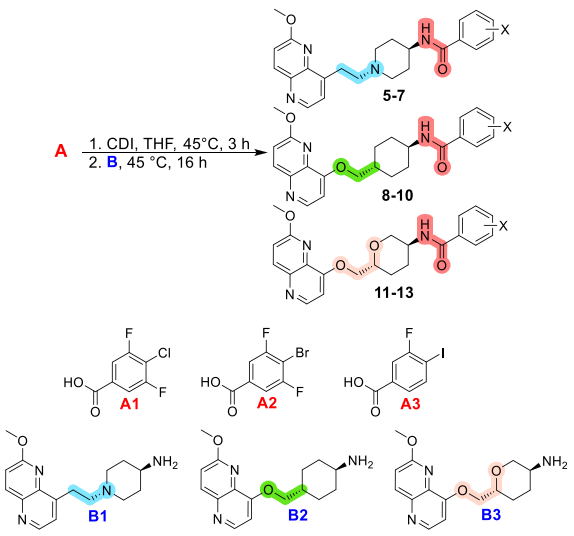

Scheme 1. Synthesis of the final compounds utilizing an amidation procedure. 1. CDI, THF 45 °C, 3 h; 2. **B**, 45 °C, 16 h.

NBTIs (**11**–**13**) being slightly less potent. The same trend was also observed in our previous study dealing with the amine containing NBTIs (Table S1) [28]. Moreover, the compounds encompassing cyclohexane linker showed a complete loss of the enzyme inhibitory and antibacterial activity when the secondary amine (e.g., **2**) was replaced with an amide (e.g., **8**–**10**).

In general, almost all of the reported compounds (e.g., **5**–**7** and **11**–**13**) show higher antibacterial potency against Gram-positive relative to Gram-negative pathogens. Evidently, the antibacterial activity of these NBTIs against wild-type *E. coli* was lower than expected considering their high on-target potency (Tables 1, 2, S2). To investigate the reason behind such a discrepancy, we opted to additionally examine their behavior on *E. coli* D22 strain with mutation in the *lpxC* gene that increases membrane permeability as well as *E. coli* N43 *AcrA* knockout strain that lacks the cell membrane efflux pumps. The MIC values on both indicate to more potent antibacterial activity for **5**–**7** and even more for **11**–**13** on N43 strain, while the activity on D22 strain was comparable (**11**–**13**) or slightly higher (**5**–**7**). This pinpoints that the permeability is an issue, however the impact of efflux appears to be even more significant, as already noted [33].

To evaluate the pharmacodynamic properties of **12**, we examined the bactericidal kinetics of the compound using a time-kill assay with planktonic methicillin-resistant *S. aureus* (ATCC 43300) and compared it to ciprofloxacin (Fig. 2A and B). Compound **12** showed a dose-dependent killing efficacy achieving bactericidal effect at 8 × MIC after 8 h of treatment, after which re-growth occurred. Ciprofloxacin showed bactericidal activity at 4 × MIC after 24 h of treatment, while at 8 × MIC bactericidal activity was achieved after 6 h of treatment and no bacterial recovery was observed after 24 h.

To determine post-antibiotic effect (PAE), *S. aureus* (MRSA strain) culture was briefly (1 h) exposed to a high concentration of **12** or ciprofloxacin (both at 8 × MIC), and bacterial recovery was followed for 8 h. The duration of PAE for compound **12** was determined to be 3 h, which is similar to the duration of PAE for ciprofloxacin (Fig. 2C).

The development of resistance to **12** was examined by serial MIC determinations of increasing passages of MRSA. As shown in Fig. 2D, an eight-fold change in MIC was observed during the first seven passages in both treatments, followed by stabilization of the MIC value. Although the MIC values increased, the MIC of **12** remained lower than that of ciprofloxacin (0.128 and 2 μg/mL, respectively), whereas the rate of resistance development to these two compounds was comparable.

The *in vitro* safety profile was determined by the blockage of hERG potassium channel and metabolic activity assessment on HepG2 liver cancer cell lines, which was assessed by compounds' effect on cell metabolic activity (Table 1). In general, the cytotoxic IC_{50} values against the HepG2 cell line were higher compared to the corresponding *S. aureus* MIC values (in μM, Table 2). The highest cytotoxicity on HepG2 cells was observed for compound **11** (IC_{50} HepG2 = 9.06 μM), while the MIC against *S. aureus* was 33 folds lower (MIC *S. aureus* = 0.269 μM; Table 2). For compounds **5**–**10**, and **12** the residual metabolic activity was >50% at a concentration of 50 μM, therefore the cytotoxic IC_{50} was not determined. As shown in Table 1, for compounds containing piperidine linkers (**1** and **5**–**7**), only the replacement of the secondary amine (e.g., **1**) with an amide (e.g., **5**) is apparently not sufficient to decrease hERG inhibition. The hERG inhibitory activity of **6** that contains amide linker (IC_{50} hERG = 0.122 μM) is even stronger compared to **1** comprising amine linker (IC_{50} hERG = 0.296 μM). This is in line with our previous observation that the tertiary amine fits the pharmacophore for hERG inhibitors, so potent hERG inhibition was not unexpected.[28] However, the opposite was observed for compounds with cyclohexane and tetrahydropyran linker. In both cases the replacement of amine (**2**, **3**) with an amide (**9**, **12**) results in at least 6-fold reduction of the hERG inhibition proving that not only tertiary, but also the secondary amine in NBTI structure should be replaced to avoid hERG inhibition, although the secondary amine seems not to have a tremendous impact on the hERG inhibition (Table 1 and S1). A similar trend was observed with the series of dioxane-linked NBTIs by Lu et al. [29]. The paramount influence of the tertiary amine on hERG inhibition is best seen when comparing **5**–**7** to **8**–**13**, where removal of the piperidine tertiary amine yet retaining the linker polarity led to 160–300 fold weaker hERG inhibition. This confirms that the tertiary amine at specific position in the NBTI's linker is a key structural determinant for their hERG inhibitory activity [28]. It should be stressed, however that exclusion of the amine from the structure notably impacts the solubility of NBTIs. This is exemplified with the compounds **8**–**11** having slight solubility issues above 100 μM and consequently their hERG IC_{50}s were not determined. Although the amide-containing compounds exhibit similar hERG inhibitory activity as gepotidacin, it should be stressed that reported gepotidacin's hERG inhibitory activity is determined by utilizing patch-clamp assay (hERG IC_{50} = 588 μg/mL) [34]. Since, these compounds did not exhibit any significant on-target potency and antibacterial activity, they were discarded from further studies.

An optimal balance between the antibacterial and hERG inhibitory activity should be achieved for an NBTI to be an effective antimicrobial lead compound, which is represented by the hERG IC_{50}/MIC ratio. The hERG IC_{50}/MIC ratio for *S. aureus* and MRSA QA-11.7 is shown in Table 2. For clarity, we set an arbitrary threshold for the hERG IC_{50}/MIC ratio at 100 for compounds that will be used in *in vivo* studies, and therefore the tetrahydropyran-linked NBTI analogs containing an amide (**11**–**13**) exhibited optimal hERG IC_{50}/MIC ratios (>100) that are even higher than that for gepotidacin.

All these data point to an important conclusion that basicity and/or polarity of the linker part should be retained as much as possible to preserve the broad-spectrum antibacterial activity and to preserve compounds' solubility. Unfortunately, this is in sharp contrast with structural requirements for evading hERG inhibition, where tertiary amine in the linker part should be avoided by all means. With retained secondary amine in the linker, we succeed to obtain the lead compound **4** with broad-spectrum antibacterial activity as well as suitable hERG IC_{50}/MIC ratio for Gram-positive bacteria [28]. The substitution of secondary amine with an amide significantly decreased antibacterial activity in Gram-negative bacteria, showing that amine-deficient compounds lack activity against Gram-negative bacteria, as already predicted by Hergenrother *at el* [35]. However, in Gram-positive bacteria, some of the amide-containing representatives still showed strong antibacterial activity (e.g., *S. aureus* and MRSA) with no significant inhibition of hERG up to 100 μM.

Table 1
S. aureus and *E. coli* DNA gyrase/topoIV inhibitory potencies, human topoisomerase IIα residual activities, hERG inhibition data and cytotoxicity data on human HepG2 cell line.

Cmpd	Structure	IC_{50} (μM)[a]				Human TopoIIα (% RA at 100 μM)[d]	hERG IC_{50} (μM)[a]	HepG2 (% RA at 50 μM)[e]
		DNA gyrase[b]		topoIV[c]				
		S. aureus	*E. coli*	*S. aureus*	*E. coli*			
1*	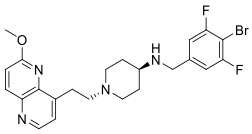	0.004 ±0.000	0.087 ±0.007	0.050 ±0.007	0.033 ±0.001	99.54 ±0.02	0.296	IC_{50} = 12 ±1.84[a]
2**	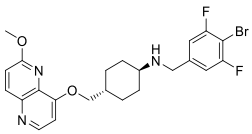	0.113 ±0.003	0.234 ±0.048	3.118 ±0.275	0.018 ±0.002	109.26 ±1.70	4.628	IC_{50} = 22 ±0.57[a]
3**	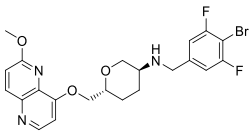	0.056 ±0.001	0.334 ±0.114	>100	0.016 ±0.005	103.89 ±2.62	16.07	68 ±8
4**	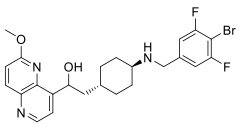	0.021 ±0.001	0.054 ±0.002	1.557 ±0.159	0.009 ±0.001	96.79 ±19.57	2.02	IC_{50} = 10 ±0.03[a]
5	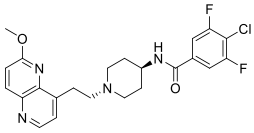	0.220 ±0.000	0.236 ±0.028	0.177 ±0.053	0.041 ±0.006	101.40 ±0.35	0.178	84 ±3
6	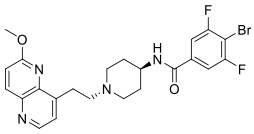	0.108 ±0.019	0.114 ±0.029	0.084 ±0.015	0.040 ±0.004	102.36 ±1.00	0.122	61 ±4
7	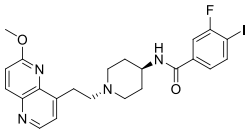	0.114 ±0.001	0.277 ±0.014	0.261 ±0.103	0.043 ±0.009	102.24 ±0.58	0.096	89 ±5
8	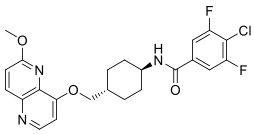	>100	>100	>100	>100	100.06 ±2.78	>30[f]	96 ±2
9	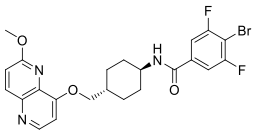	>100	>100	>100	>100	101.27 ±0.19	>30[f]	90 ±3
10	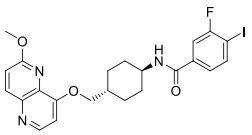	>100	>100	>100	>100	99.12 ±3.77	>30	96 ±4
11	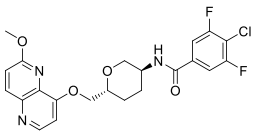	0.445 ±0.029	0.677 ±0.045	0.579 ±0.126	0.073 ±0.018	100.97 ±1.77	>30[f]	IC_{50} = 9.06 ±0.02[a]

(*continued on next page*)

Table 1 (*continued*)

Cmpd	Structure	IC_{50} (μM)[a]				Human TopoIIα (% RA at 100 μM)[d]	hERG IC_{50} (μM)[a]	HepG2 (% RA at 50 μM)[e]
		DNA gyrase[b]		topoIV[c]				
		S. aureus	*E. coli*	*S. aureus*	*E. coli*			
12	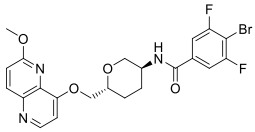	0.185 ±0.008	0.365 ±0.136	0.341 ±0.072	0.059 ±0.015	99.40 ±0.73	>30 (79%) [g]	89 ±6
13	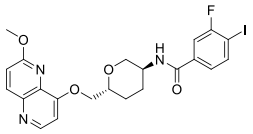	0.271 ±0.071	0.358 ±0.033	0.783 ±0.039	0.092 ±0.025	102.09 ±0.00	>30 (72%) [g]	IC_{50} = 11.24 ±3.17[a]
Gepo	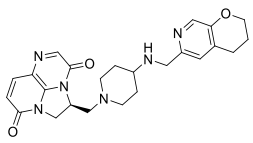	0.374 ±0.019	0.244 ±0.040	8.299 ±0.361	0.049 ±0.003	ND	>30 (68%) [g]	ND

[a] IC_{50}, mean of two independent measurements ± SD.
[b] DNA gyrase supercoiling inhibition assay.
[c] topoIV relaxation inhibition assay.
[d] Residual activity, mean ± SD of residual activity (%) at 100 μM compound from two independent experiments.
[e] %RA, mean ± SD for residual cell metabolic activity at 50 μM compound from two independent experiments.
[f] IC_{50} was not determined due to poor solubility above 100 μM.
[g] Residual activity (%) at 100 μM. ND: not determined; Gepo: gepotidacin; * [32]; ** [28].

Table 2
Antimicrobial activity (in μM) of the optimized NBTIs against a panel of Gram-positive and Gram-negative bacterial pathogens and hERG IC_{50}/MIC ratio.

Cmpd	MIC (μM)													
	1*	2**	3**	4**	5	6	7	8	9	10	11	12	13	Gepo
***S. aureus* (ATCC 29213)**	0.008	0.063	0.035	0.016	0.137	0.061	0.058	277	253	239	0.136	0.031	0.058	0.279
***E. coli* (ATCC 25922)**	1.02	8.12	34.9	1.97	69.4	63.3	240	277	64.8	239	276	252	238	2.23
***E. coli* D22**[a]	0.033	0.508	0.545	0.032	0.542	0.247	0.468	277	64.8	239	276	252	238	0.279
***E. coli* N43**[b] **(CGSC# 5583)**	0.016	0.063	0.135	0.016	0.135	0.061	0.234	277	64.8	239	0.134	0.061	0.117	0.036
***E. coli* ESBL QA:11.3**[c]	ND	8.12	>279	3.95	>278	253	>240	>277	>64.8	>239	>276	>252	>238	ND
MRSA QA-11.7[d]	0.033	0.063	0.135	<0.016	0.271	0.247	0.234	277	64.8	239	0.136	0.061	0.058	0.138
MRSAQA-12.1[e]	0.033	0.12	0.068	<0.016	0.137	0.061	0.058	277	>64.8	>239	0.136	0.031	0.058	0.279
MRSA QA-11.2	ND	0.254	0.135	0.016	0.271	0.125	0.234	>277	>64.8	>239	0.269	0.124	238	ND
K. pneumoniae	16.3	260	279	15.8	>278	>253	>240	>277	>64.8	>239	>276	>252	>238	17.8
***S. alachua* RDK 030c**	2.04	260	279	7.90	>278	>253	>240	>277	>64.8	>239	>276	>252	>238	8.92
***P. aeruginosa* RDK 184**	16.3	260	279	31.6	>278	>253	>240	>277	>64.8	>239	>276	>252	>238	17.8
***E. faecalis* DRK 057**	1.02	2.03	1.09	0.247	2.17	0.495	0.468	>277	>64.8	>239	8.62	4.07	>238	ND
A. baumannii	1.02	>260	>279	1.98	4.34	3.96	240	>277	>64.8	>239	276	252	>238	ND
hERG IC_{50}/MIC[f] ***S. aureus***	36.4	73.5	460	131	1.30	1.99	1.65	≥0.108	≥0.119	≥0.125	≥224	≥953	≥520	≥139
hERG IC_{50}/MIC[f] **MRSA QA-11.7**	9.09	73.5	119	>131	0.656	0.493	0.410	≥0.108	≥0.119	≥0.125	≥224	≥492	≥520	≥281

[a] With a mutation in the *lpxC* gene that increases membrane permeability.
[b] With *AcrA* knock-out (cell membrane efflux pump).
[c] Resistant to: ampicillin, cefotaxime, ceftazidime, chloramphenicol, ciprofloxacin, colistin, gentamicin, meropenem, nalidixic acid, sulfamethoxazole, tetracycline, trimethoprim, cefepime, cefoxitin, imipenem.
[d] Resistant to cefoxitin, ciprofloxacin, clindamycin, erythromycin, tetracycline, thiamulin, trimethoprim.
[e] Resistant to cefoxitin, gentamicin, kanamycin, rifampicin, streptomycin, sulfamethoxazole, tetracycline. ATCC, American Type Culture Collection; CGSC, Coli Genetic Stock Centre; QA, Quality Assurance.
[f] hERG and MIC values are in μM; ND: not determined; Gepo: gepotidacin. * [32]; ** [28].

2.4. Zebrafish toxicity study

In order to determine the average lethal concentrations (LC_{50}s) and the highest non-toxic doses, zebrafish embryos were incubated with increasing concentrations of the tested compounds (0.39, 0.78, 1.56, 3.12, 6.25, 12.5, and 25 μg/mL) and inspected for the presence of apical endpoints daily. Zebrafish is a suitable model for preclinical toxicity studies, owing to its genetic, molecular, and immunological similarity to humans and highly correlated response to pharmaceuticals [36]. Additionally, zebrafish embryos express orthologue to hERG, are sensitive towards a range of QT-prolonging drugs and can be utilized to assess the effects of chemicals on hERG [37]. The majority of compounds, with the exception of **12**, exhibited lethal effects, cardiotoxicity, and hepatotoxicity at higher doses (Fig. 3). **1** and **2** exhibited acute toxicity at two highest tested doses and signs of cardiotoxicity (pericardial edema and irregular heart beat), hepatotoxicity, and intestinal toxicity at lower doses. At doses lower than 1.56 μg/mL, **2** showed no toxic effects in zebrafish embryos. **3** exhibited acute and developmental toxicity (cardiotoxicity and other signs of toxicity such as scoliosis and tail malformation) at doses higher than 1.56 μg/mL, while no toxic effects were

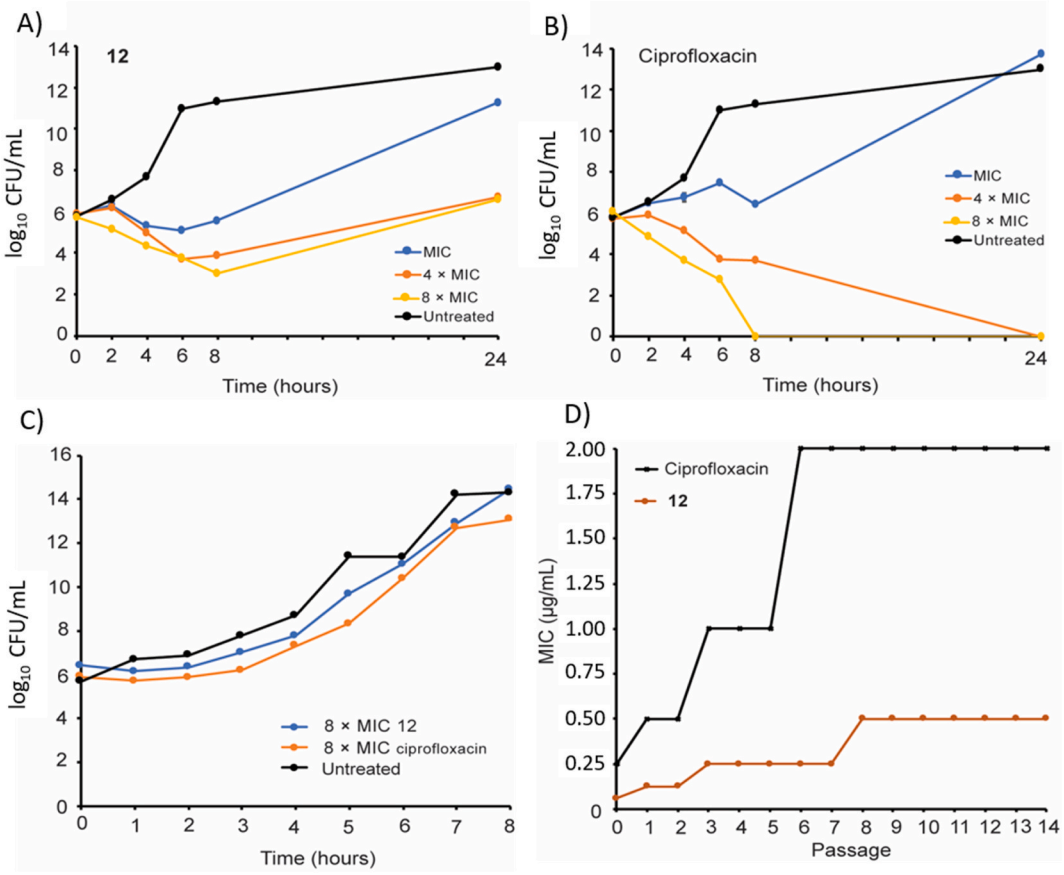

Fig. 2. A) Time-kill curve of 12 against MRSA ATCC 43300; B) Time-kill curve of ciprofloxacin against MRSA ATCC 43300; C) PAE: Regrowth curves of MRSA ATCC 43300 exposed to 12 or ciprofloxacin for 1 h; D) Resistance development study of 12 and ciprofloxacin against MRSA ATCC 43300 as shown by MIC increase over a period of 14 passages.

observed at lower doses. **4** exhibited cardiotoxicity (irregular heart beat) at doses higher than 3.125 μg/mL. **6** showed hepatotoxic (observed at 25 μg/mL) and cardiotoxic (irregular heartbeat) effects at doses higher than 1.56 μg/mL. **12** exhibited no toxic effect, indicating that **12** does not inhibit hERG potassium channels and is not cardiotoxic to zebrafish models.

Compounds (**3**, **4**, and **12**) containing different linker, having hERG IC_{50}/MIC ratio above 100 and showing slight or no toxic effect on zebrafish models were selected as promising lead compounds for *in vivo* efficacy studies to treat *S. aureus*/MRSA infections.

2.5. *In vivo assays*

Compounds **3**, **4**, and **12** that have suitable hERG IC_{50}/MIC ratio for MRSA QA-11.7 (Table 3) and no toxic effect on zebrafish models were further used in *in vivo* studies. The mouse tolerability for the selected NBTIs was initially assessed, followed by neutropenic mouse thigh infection study.

Mouse tolerability studies. The results of the mouse tolerability assessment for **3** and **4** show that these compounds procure convulsions after intravenous (IV) administration (Supporting information, Table S3). However, after intraperitoneal (IP) administration convulsions were not observed, which allowed a safe mode of administration for further *in vivo* assaying of the test compounds. Relative to the IP route of administration, the IV route usually outcomes in a highest bioavailability of the drug [38] that consequently is manifested by convulsion in treated animals. Detailed toxicological profiling was not performed as it was out of scope of this study.

MRSA neutropenic thigh infection model. The *in vivo* efficacy study of selected compounds (**3**, **4**, and **12**) and gepotidacin (as a positive control) was conducted in two regimens, i.e., BID regimen – fixed dose every 12 h (Supporting information, Table S4 and Fig. S1) and QID regimen – fixed dose every 6 h (Table 3 and Fig. 4) by using neutropenic mice infected with MRSA strain BAA-1717 (TCH 1516). We used BID regimen as a preliminary study to estimate the appropriate doses (Supporting information, Table S4 and Fig. S1). Mice receiving compounds **3**, **4** or **12** delivered IP demonstrated inhibition of bacterial growth in a dose dependent manner. QID regimen led to higher overall dose received that had a more pronounced effect on change in $\log_{10}$ CFU on gram of thigh (Fig. 4). Untreated mice demonstrated a 2.96 $\log_{10}$ CFU increase from initiation of treatment to study termination (26 h). Compounds **3** and **4** demonstrated dose dependent inhibition of bacterial growth in two doses (20 and 40 mg/kg QID) with 40 mg/kg dose exhibiting a >3.85 $\log_{10}$ CFU reduction from the 26 h infection controls. This proves that all 3 compounds outperform gepotidacin in MRSA model since mice receiving 50 mg/kg administered IP, QID dose (slightly higher dose) of gepotidacin exhibited a 2.34 $\log_{10}$ CFU reduction from the 26 h infection controls. Interestingly, CFUs collected from the animals dosed by **4** showed smaller colony size, which suggests a postantibiotic effect [39]. Comparison of the *in vivo* efficacy of **12** leads to an interesting observation that both 20 and 40 mg/kg QID doses lead to a similar reduction in CFU after 26 h. This can probably be attributed to a lower solubility of **12**, so our further efforts will be dedicated to improve physicochemical properties of the lead. On the other hand, higher lipophilicity of **12** might lead to a higher plasma protein binding, which could be employed as depot to increase compound's plasma half-life and thus diminish the number of doses given to achieve therapeutically useful antibacterial effect. Both aspects will be tackled in the continuation of our studies.

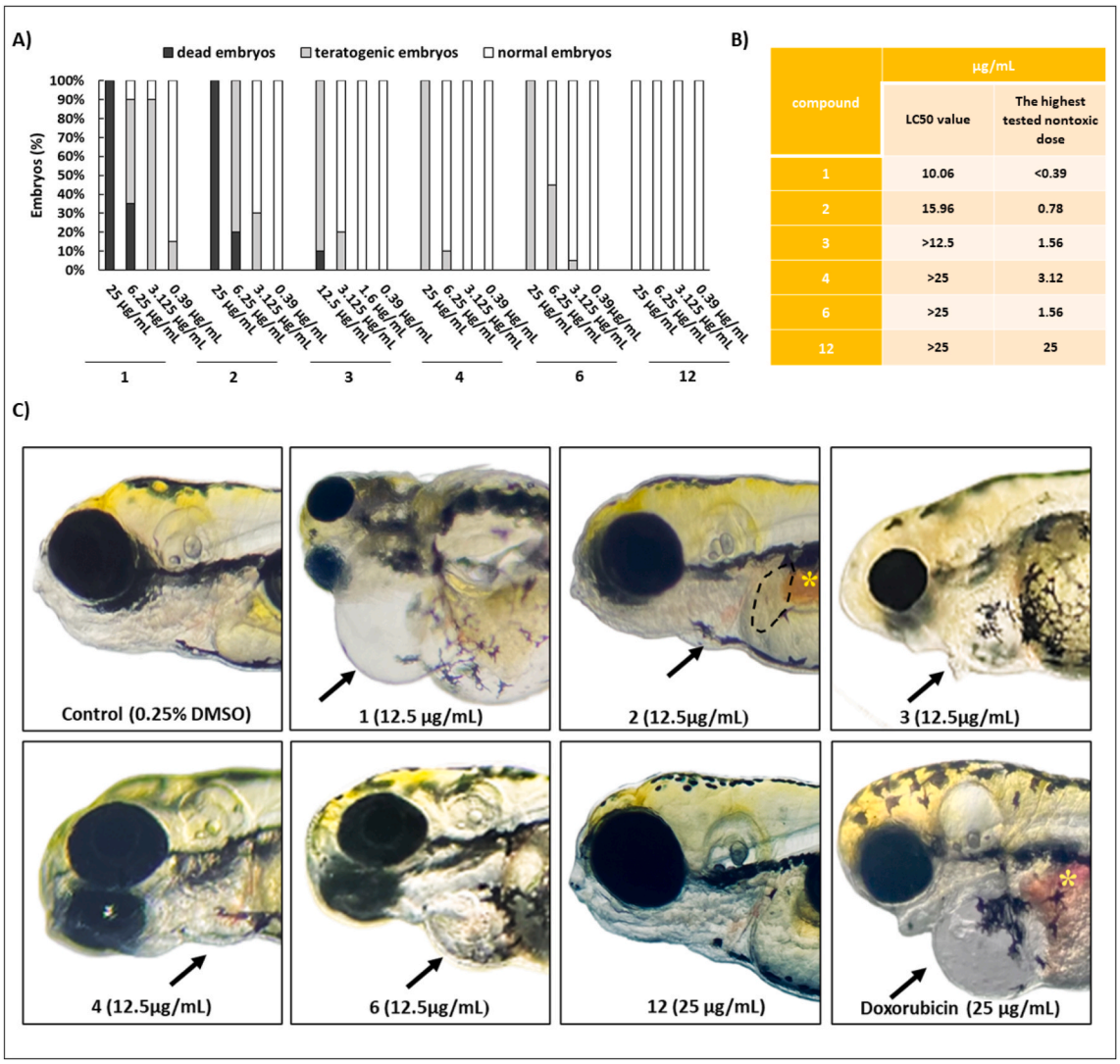

compound	µg/mL	
	LC50 value	The highest tested nontoxic dose
1	10.06	<0.39
2	15.96	0.78
3	>12.5	1.56
4	>25	3.12
6	>25	1.56
12	>25	25

Fig. 3. *In vivo* toxicity of the compounds was evaluated in wild-type zebrafish embryos. A) Dose dependent toxicity of the compounds. B) Average lethal concentrations (LC_{50}s) and the highest tested non-toxic doses of the compounds. C) Developmental toxicity signs in zebrafish embryos treated with compounds (arrow: pericardial edema, dotted: liver necrosis, asterisk: intestinal toxicity).

3. Conclusion

In summary, the optimized, focused series of amide-containing NBTIs represented here is expanding the SAR guidelines to reduce the hERG inhibition, while retaining their antibacterial effect. In our previous study, we pointed out the importance of removing the tertiary amine from the structure (e.g., piperidine-linked NBTIs), i.e., a key determinant towards diminishing the hERG inhibitory activity [28]. Here, we demonstrated that substituting the secondary amine with an amide in the linker moiety undoubtedly leads to even further decrease in the hERG inhibition for NBTIs comprising non-piperidine linkers (e.g., cyclohexane and tetrahydropyran). Among them, compound **12** proved to be a potent inhibitor of bacterial type II topoisomerases on isolated enzymes, it showed potent antibacterial activity especially against MRSA strains (QA-11.7, QA-12.1, and QA-11.2), and exhibited no significant hERG inhibition and no cardiotoxicity on zebrafish model compared to our previous NBTIs [28,32]. Moreover, **12** also demonstrated high *in vivo* efficacy in MRSA neutropenic mouse thigh infection model. We conclude that **12** is a promising lead compound for further optimization to maintain the desired antibacterial activity and acceptable safety profile. It represents a new bacterial type II topoisomerase inhibitor and we are confident in its potential for combating bacterial resistance caused by Gram-positive bacteria.

4. Experimental section

4.1. General chemical methods

Starting materials, reagents, and solvents were obtained from commercial sources and used without additional preparation. Thin layer chromatography (TLC) analysis was used for reaction progress, product isola-tion, and solvent selection for purification. Analytical TLC was performed on Merck 60 F254 (0.25 mm) silica gel plates, and products were visualized with UV light and spray reagents. Final products were purified by column chromatography on silica gel 60 (particle size 240–400 mesh). Compounds were eluted using an optimized gradient of dichloromethane:methanol. Purity and identity were further confirmed by NMR spectroscopy. The resonance frequency for ^{1}H and ^{13}C in NMR was recorded at 400 MHz and 100 MHz using an AVANCE III 400 spectrometer (Bruker Corporation, Billerica, MA, USA) in $CDCl_3$. Chemical shifts (δ) are given in parts per million (ppm), with respect to the deuterated solvent as the internal standard (δ_H: $CDCl_3$ 7.26 ppm), and coupling constants (J) in hertz (Hz). Peak multiplications are given as follows: singlet (s), doublet (d), doublet of doublets (dd), triplet (t),

Table 3
In vivo neutropenic mouse thigh infection data.

Group ID	Dose (mg/kg)	Total Dose (mg/kg)	Route/regimen	Average log_{10} CFU/gr of thigh	Change in log_{10} CFU/gr of thigh from	
					2 h Controls	26 h Controls
2 h. Infection Control	N/A	N/A	N/A	5.90 ±0.17	/	−2.96
26 h. Infection Control	N/A	N/A	N/A	8.85 ±0.22	2.96	/
3	20	80	IP/QID	7.25 ±0.51	1.35	−1.60
	40	160	IP/QID	4.93 ±0.04	−0.97	−3.92
4	20	80	IP/QID	7.54 ±0.27	1.64	−1.31
	40	160	IP/QID	4.74 ±0.16	−1.16	−4.12
12	20	80	IP/QID	5.43 ±1.19	−0.47	−3.43
	40	160	IP/QID	5.01 ±0.08	−0.89	−3.85
Gepo	50	200	IP/QID	6.52 ±1.49	0.62	−2.34

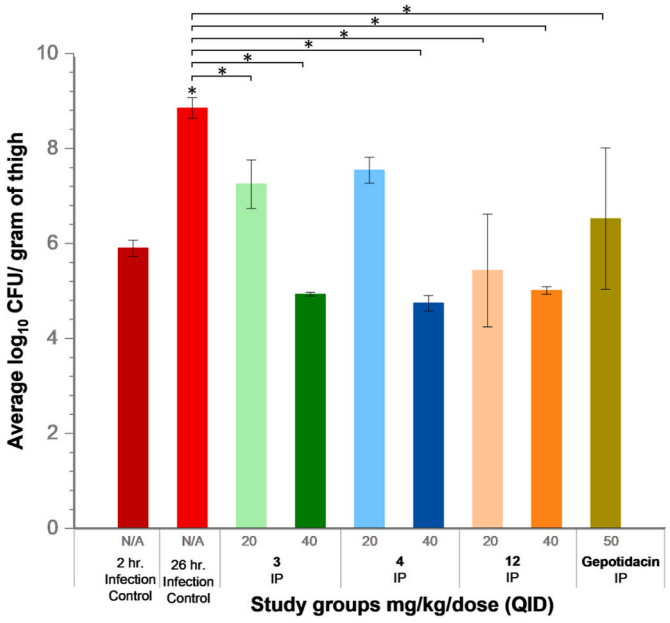

Fig. 4. *In vivo* efficacy of selected NBTI compounds utilizing neutropenic mouse thigh infection model (QID regimen). Neutropenic mice infected with MRSA strain BAA-1717 (TCH 1516) were treated with **3**, **4**, **12**, or gepotidacin to evaluate their antibacterial efficacy. The plot depicts the average log_{10} CFU/gr of thigh for three selected NBTI compounds (**3**, **4**, and **12**) in two different doses (20 and 40 mg/kg) injected IP four times (every 6 h, after 2 h of infection control) and gepotidacin as a positive control injected as a single dose (50 mg/kg) four times (every 6 h). The error bars represent standard errors of the mean for each dose group of treated animals (n = 4), *, $p < 0.05$ (one-way ANOVA, with Bonferroni corrections, followed by *t*-test).

multiplet (m). High-resolution mass spectra were recorded using a LC-MS/MS system (Q Exactive Plus; Thermo Scientific, MA, USA). Unless otherwise indicated, all compounds had a purity of ≥95% as determined by HPLC on an 1100 system (Thermo Scientific Dionex UltiMate 3000 (Thermo Fisher Scientific, Inc.). For the general method, a Waters Acquity UPLC® HSS C18 SB column (2.1 × 50 mm, 1.8 μm) thermostated at 40 °C was used, with: injection volume, 5 μL; sample, 0.1–0.2 mg/mL in MeOH; flow rate, 0.4 mL/min; detector λ, 220 and 254 nm; mobile phase A: 0.1% TFA (v/v) in water; mobile phase B: MeCN. Gradient: 0–2 min, 20% B; 2–5 min, 20%–90% B; 5–8 min, 90% B.

4.1.1. Synthesis of intermediates

6-methoxy-1,5-naphthyridin-4(1H)-one, (1R, 4R)-1-(2-(6-methoxy-1,5-naphthyridin-4-yl)ethyl)piperidin-4-amine (**B1**), (1R, 4R)-4-(((6-methoxy-1,5-naphthyridin-4-yl)oxy)methyl)cyclohexan-1-amine (**B2**) and (3R, 6S)-6-(((6-methoxy-1,5-naphthyridin-4-yl)oxy)methyl)tetrahydro-2H-pyran-3-amine (**B3**) were synthetized by the procedure from our previously published publication [28].

4.1.2. General amidation procedure

The suitable *p*–halogenated benzoic acid (**A1**, **A2** or **A3**) (1.5 eq) and 1,1′-carbonyldiimidazole (CDI) (1.5 eq) were dissolved in dry THF (1 mL) under argon atmosphere. The reaction mixture was stirred for 3 h at 45 °C under argon atmosphere. Corresponding amine (**B1**, **B2** or **B3**) (1 eq) dissolved in THF was added, and the reaction was stirred at 45 °C 16 h. Then the solvent was evaporated and water (20 mL) was added to the crude product and suspension was extracted with 3 × 10 mL of DCM. The combined organic phases were dried over Na_2SO_4, filtered and evaporated. The crude product was purified by flash chromatography on silica gel to afford the title compounds (**5**–**13**).

4.1.3. Synthesis of the final compounds

4.1.3.1. (1R,4R)-4-Chloro-3,5-difluoro-N-(1-(2-(6-methoxy-1,5-naphthyridin-4-yl)ethyl)piperidin-4-yl)benzamide (5). The title compound was obtained according to general procedure using **B1** (143 mg, 0.50 mmol, 1 eq), 4-chloro-3,5-difluorobenzoic acid (144 mg, 0.75 mmol, 1.5 eq), CDI (121 mg, 0.75 mmol, 1.5 eq) and dry THF (4 mL). The crude product was purified by flash column chromatography (SiO_2, dichlorometane: methanol = 15:1) to afford **5** (186 mg, 80%). ^{1}H NMR (400 MHz, $CDCl_3$): δ 8.66 (d, J = 4.5 Hz, 1H), 8.18 (d, J = 9.0 Hz, 1H), 7.43–7.37 (m, 3H), 7.12 (d, J = 9.0 Hz, 1H), 6.04 (d, J = 7.6 Hz, 1H), 4.08 (s, 3H), 4.04–3.92 (m, 1H), 3.43–3.32 (m, 2H), 3.07 (d, J = 11.9 Hz, 2H), 2.85–2.79 (m, 2H), 2.35–2.26 (m, 2H), 2.09–2.04 (m, 2H), 1.68–1.46 (m, 2H) ppm. ^{13}C NMR (100 MHz, $CDCl_3$): δ 163.85, 161.58, 158.99 (dd, J = 252.6, 3.3 Hz), 147.77, 146.63, 141.63, 141.09, 140.46, 134.89 (t, J = 7.5 Hz), 124.33, 116.47, 113.47, 110.87 (dd, J = 23.8, 2.2 Hz), 58.40, 53.80, 52.35, 47.85, 32.41, 28.56 ppm. HRMS: *m/z*: calcd for $C_{23}H_{24}ClF_2N_4O_2$ $[M+H]^+$: 461.1550, found: 461.1528. HPLC: t_R = 3.720 min (99% at 220 nm).

4.1.3.2. (1R,4R)-4-Bromo-3,5-difluoro-N-(1-(2-(6-methoxy-1,5-naphthyridin-4-yl)ethyl)piperidin-4-yl)benzamide (6). The title compound was obtained according to general procedure using **B1** (144 mg, 0.50 mmol, 1 eq), 4-bromo-3,5-difluorobenzoic acid (179 mg, 0.75 mmol, 1.5 eq),

CDI (122 mg, 0.75 mmol, 1.5 eq) and dry THF (4 mL). The crude product was purified by flash column chromatography (SiO_2, dichlorometane: methanol = 15:1) to afford **6** (175 mg, 69%). ^{1}H NMR (400 MHz, $CDCl_3$): δ 8.66 (d, J = 4.5 Hz, 1H), 8.18 (d, J = 9.0 Hz, 1H), 7.41 (d, J = 4.5 Hz, 1H), 7.37–7.31 (m, 2H), 7.11 (d, J = 9.0 Hz, 1H), 5.94 (d, J = 7.7 Hz, 1H), 4.07 (s, 3H), 4.05–3.93 (m, 1H), 3.41–3.32 (m, 2H), 3.06 (d, J = 11.9 Hz, 2H), 2.86–2.76 (m, 2H), 2.37–2.25 (m, 2H), 2.10–2.00 (m, 2H), 1.63–1.49 (m, 2H) ppm. ^{13}C NMR (100 MHz, $CDCl_3$): δ 163.92, 161.59, 158.85, 147.81, 146.64, 141.66, 141.11, 140.50, 124.34, 116.48, 110.87, 110.62 (d, J = 2.4 Hz), 58.43, 53.82, 52.36, 47.84, 32.44, 28.59 ppm. Due to possible overlap or short relaxation time one carbon is missing. HRMS: *m/z*: calcd for $C_{23}H_{24}BrF_2N_4O_2$ $[M+H]^+$: 505.1045, found: 505.1022. HPLC: t_R = 3.803 min (99% at 220 nm).

4.1.3.3. (1R,4R)-3-Fluoro-4-iodo-N-(1-(2-(6-methoxy-1,5-naphthyridin-4-yl)ethyl)piperidin-4-yl)benzamide (7). The title compound was obtained according to general procedure using **B1** (144 mg, 0.50 mmol, 1 eq), 4-iodo-3-fluorobenzoic acid (201 mg, 0.75 mmol, 1.5 eq), CDI (122 mg, 0.75 mmol, 1.5 eq) and dry THF (4 mL). The crude product was purified by flash column chromatography (SiO_2, dichlorometane: methanol = 15:1) to afford **7** (101 mg, 38%). ^{1}H NMR (400 MHz, DMSO-d_6): δ 8.68 (d, J = 4.4 Hz, 1H), 8.37 (d, J = 7.7 Hz, 1H), 8.25 (d, J = 9.0 Hz, 1H), 7.96 (dd, J = 8.1, 6.5 Hz, 1H), 7.68 (dd, J = 9.2, 1.9 Hz, 1H), 7.60 (d, J = 4.5 Hz, 1H), 7.49 (dd, J = 8.2, 1.9 Hz, 1H), 7.26 (d, J = 9.0 Hz, 1H), 4.04 (s, 3H), 3.81–3.69 (m, 1H), 3.30 (d, J = 7.8 Hz, 2H), 3.03 (d, J = 11.4 Hz, 2H), 2.74 (t, J = 7.4 Hz, 2H), 2.12 (t, J = 11.0 Hz, 2H), 1.78 (d, J = 9.7 Hz, 2H), 1.59–1.43 (m, 2H) ppm. ^{13}C NMR (100 MHz, DMSO-d_6): δ 164.04 (d, J = 1.9 Hz), 161.49 (d, J = 242.7 Hz), 161.40, 148.23, 146.72, 141.41, 141.04, 140.85, 139.73 (d, J = 1.6 Hz), 137.47 (d, J = 6.3 Hz), 125.50 (d, J = 3.2 Hz), 125.06, 116.59, 114.65 (d, J = 25.5 Hz), 86.55 (d, J = 26.0 Hz), 58.25, 53.87, 52.52, 47.65, 31.89, 28.01 ppm. HRMS: *m/z*: calcd for $C_{23}H_{25}FIN_4O_2$ $[M+H]^+$: 535.1000, found: 505.0976. HPLC: t_R = 5.417 min (97% at 220 nm).

4.1.3.4. (1R,4R)-4-Chloro-3,5-difluoro-N-(4-(((6-methoxy-1,5-naphthyridin-4-yl)oxy)methyl)cyclohexyl)benzamide (8). The title compound was obtained according to general procedure using **B2** (100 mg, 0.35 mmol, 1 eq), 4-chloro-3,5-difluorobenzoic acid (101 mg, 0.52 mmol, 1.5 eq), CDI (85 mg, 0.52 mmol, 1.5 eq) and dry THF (4 mL). The crude product was purified by flash column chromatography (SiO_2, dichlorometane: methanol = 30:1) to afford **8** (34 mg, 21%). ^{1}H NMR (400 MHz, $CDCl_3$): δ 8.61 (d, J = 5.2 Hz, 1H), 8.16 (d, J = 9.0 Hz, 1H), 7.39 (d, J = 7.0 Hz, 2H), 7.12 (d, J = 9.1 Hz, 1H), 6.90 (d, J = 5.2 Hz, 1H Ar–H), 5.88 (d, J = 7.1 Hz, 1H), 4.11 (s, 3H), 4.07 (d, J = 6.4 Hz, 2H), 4.04–3.94 (m, 1H), 2.18 (dd, J = 28.7, 9.8 Hz, 4H), 2.10–1.97 (m, 1H), 1.48–1.27 (m, 4H) ppm. ^{13}C NMR (100 MHz, $CDCl_3$): 163.72, 161.69, 160.02, 159.04 (dd, J = 252.7, 3.2 Hz), 148.97, 142.82, 140.18, 135.03 (t, J = 7.4 Hz), 134.50, 116.71, 110.83 (dd, J = 23.7, 2.1 Hz), 105.16, 73.52, 53.78, 49.63, 36.90, 32.60, 28.48 ppm. Due to possible overlap or short relaxation time one carbon is missing. HRMS: *m/z*: calcd for $C_{23}H_{23}ClF_2N_3O_3$ $[M+H]^+$: 462.1391, found: 462.1370. HPLC: t_R = 4.480 min (98% at 220 nm).

4.1.3.5. (1R,4R)-4-Bromo-3,5-difluoro-N-(4-(((6-methoxy-1,5-naphthyridin-4-yl)oxy)methyl)cyclohexyl)benzamide (9). The title compound was obtained according to general procedure using **B2** (100 mg, 0.35 mmol, 1 eq), 4-bromo-3,5-difluorobenzoic acid (124 mg, 0.52 mmol, 1.5 eq), CDI (85 mg, 0.52 mmol, 1.5 eq) and dry THF (4 mL). The crude product was purified by flash column chromatography (SiO_2, dichlorometane: methanol = 30:1) to afford **9** (45 mg, 26%). ^{1}H NMR (400 MHz, DMSO-d_6): δ 8.14 (d, J = 5.1 Hz, 1H), 8.04 (d, J = 7.7 Hz, 1H), 7.74 (d, J = 9.0 Hz, 1H), 7.28 (d, J = 7.9 Hz, 2H), 6.80–6.73 (m, 2H), 3.65 (d, J = 6.1 Hz, 2H), 3.56 (s, 3H), 3.37–3.27 (m, 1H), 1.59–1.42 (m, 5H), 1.03–0.77 (m, 4H) ppm. ^{13}C NMR (100 MHz, DMSO-d_6): δ 162.19, 160.69, 159.35, 158.99 (dd, J = 246.9, 4.1 Hz), 149.07, 142.07, 140.11, 136.50 (t, J = 7.4 Hz), 133.74, 116.16, 111.32 (dd, J = 24.5, 2.3 Hz), 105.84, 100.15 (t, J = 24.9 Hz), 73.00, 53.26, 48.98, 36.26, 31.42, 27.90 ppm. HRMS: *m/z*: calcd for $C_{23}H_{23}BrF_2N_3O_3$ $[M+H]^+$: 506.0885, found: 506.0868. HPLC: t_R = 4.510 min (97% at 220 nm).

4.1.3.6. (1R,4R)-3-Fluoro-4-iodo-N-(4-(((6-methoxy-1,5-naphthyridin-4-yl)oxy)methyl)cyclohexyl)benzamide (10). The title compound was obtained according to general procedure using **B2** (100 mg, 0.35 mmol, 1 eq), 4-iodo-3-fluorobenzoic acid (139 mg, 0.52 mmol, 1.5 eq), CDI (85 mg, 0.52 mmol, 1.5 eq) and dry THF (4 mL). The crude product was purified by flash column chromatography (SiO_2, dichlorometane: methanol = 20:1) to afford **10** (49 mg, 26%). ^{1}H NMR (400 MHz, DMSO-d_6): δ 14.52 (s, CF_3COOH), 9.07 (d, J = 6.2 Hz, 1H), 8.41 (d, J = 9.0 Hz, 1H), 7.95–7.89 (m, 1H), 7.70 (dd, J = 26.7, 7.5 Hz, 2H), 7.53 (dd, J = 35.9, 8.4 Hz, 2H), 4.38 (d, J = 3.8 Hz, 2H), 4.06 (s, 3H), 3.82–3.72 (m, 1H), 2.04–1.89 (m, 5H), 1.45–1.28 (m, 4H) ppm. Due poor solubility CF_3COOH was added. ^{13}C NMR (100 MHz, DMSO-d_6): δ 166.50, 163.72, 162.84, 161.35 (d, J = 242.6 Hz), 158.52 (q, J = 38.9 Hz, CF_3COOH), 143.61, 139.49, 137.38 (d, J = 6.4 Hz), 133.51 (d, J = 24.6 Hz), 132.37, 125.24 (d, J = 2.6 Hz), 121.07, 115.22 (q, J = 287.8 Hz, CF_3COOH), 114.46 (d, J = 25.4 Hz), 110.93, 106.65, 86.08 (d, J = 25.9 Hz),75.61, 54.26, 48.83, 36.35, 31.57, 27.93 ppm. Due poor solubility CF_3COOH was added. HRMS: *m/z*: calcd for $C_{23}H_{24}FIN_3O_3$ $[M+H]^+$: 536.0841, found: 536.0816. HPLC: t_R = 4.473 min (96% at 220 nm).

4.1.3.7. (3R,6S)-4-Chloro-3,5-difluoro-N-(6-(((6-methoxy-1,5-naphthyridin-4-yl)oxy)methyl)tetrahydro-2H-pyran-3-yl)benzamide (11). The title compound was obtained according to general procedure using **B3** (96 mg, 0.33 mmol, 1 eq), 4-chloro-3,5-difluorobenzoic acid (96 mg, 0.50 mmol, 1.5 eq), CDI (81 mg, 0.50 mmol, 1.5 eq) and dry THF (4 mL). The crude product was purified by flash column chromatography (SiO_2, dichlorometane: methanol = 20:1) to afford **11** (138 mg, 90%). ^{1}H NMR (400 MHz, DMSO-d_6): δ 8.60 (d, J = 5.2 Hz, 1H), 8.48 (d, J = 7.4 Hz, 1H, 8.20 (d, J = 9.0 Hz, 1H), 7.78 (d, J = 7.9 Hz, 2H), 7.25–7.22 (m, 2H), 4.34–4.23 (m, 2H), 4.02 (s, 3H), 3.99–3.92 (m, 2H), 3.85–3.79 (m, 1H), 3.27–3.19 (m, 1H), 2.11–1.92 (m, 2H), 1.76–1.61 (m, 2H) ppm. ^{13}C NMR (100 MHz, DMSO-d_6): δ 162.75, 160.73, 159.17, 157.78 (dd, J = 249.0, 3.1 Hz), 149.01, 142.15, 140.13, 134.94 (t, J = 7.7 Hz), 133.64, 116.23, 111.59 (dd, J = 23.2, 2.4 Hz), 106.09, 74.90, 71.10, 69.50, 53.32, 46.08, 28.51, 26.78 ppm. Due to possible overlap or short relaxation time one carbon is missing. HRMS: *m/z*: calcd for $C_{22}H_{21}ClF_2N_3O_4$ $[M+H]^+$: 464.1183, found: 464.1164. HPLC: t_R = 4.190 min (95% at 220 nm).

4.1.3.8. (3R,6S)-4-Bromo-3,5-difluoro-N-(6-(((6-methoxy-1,5-naphthyridin-4-yl)oxy)methyl)tetrahydro-2H-pyran-3-yl)benzamide (12). The title compound was obtained according to general procedure using **B3** (96 mg, 0.33 mmol, 1 eq), 4-bromo-3,5-difluorobenzoic acid (118 mg, 0.50 mmol, 1.5 eq), CDI (81 mg, 0.50 mmol, 1.5 eq) and dry THF (4 mL). The crude product was purified by flash column chromatography (SiO_2, dichlorometane: methanol = 20:1) to afford **12** (115 mg, 68%). ^{1}H NMR (400 MHz, DMSO-d_6): δ 8.61 (d, J = 5.2 Hz, 1H), 8.48 (d, J = 7.4 Hz, 1H), 8.20 (d, J = 9.0 Hz, 1H), 7.73 (d, J = 7.5 Hz, 2H), 7.31–7.21 (m, 2H), 4.36–4.19 (m, 2H), 4.02 (s, 3H), 3.98–3.90 (m, 2H), 3.87–3.78 (m, 1H), 3.28–3.17 (m, 1H), 2.09–1.93 (m, 2H), 1.74–1.62 (m, 2H) ppm. ^{13}C NMR (100 MHz, DMSO-d_6): δ 163.34, 161.20, 159.64, 159.47 (dd, J = 246.9, 4.4 Hz), 149.49, 142.62, 140.61, 136.48 (t, J = 7.9 Hz), 134.11, 116.71, 111.87 (dd, J = 24.5, 2.6 Hz), 106.57, 100.91 (t, J = 25.0 Hz), 75.3, 71.57, 69.95, 53.80, 46.52, 28.97, 27.23. HRMS: *m/z*: calcd for $C_{22}H_{21}BrF_2N_3O_4$ $[M+H]^+$: 508,0605 found: 508.0656. HPLC: t_R = 5.847 min (96% at 220 nm).

4.1.3.9. (3R,6S)-3-Fluoro-4-iodo-N-(6-(((6-methoxy-1,5-naphthyridin-4-yl)oxy)methyl)tetrahydro-2H-pyran-3-yl)benzamide (13). The title

compound was obtained according to general procedure using **B3** (96 mg, 0.33 mmol, 1 eq), 4-iodo-3-fluorobenzoic acid (132 mg, 0.50 mmol, 1.5 eq), CDI (81 mg, 0.50 mmol, 1.5 eq) and dry THF (4 mL). The crude product was purified by flash column chromatography (SiO_2, dichlorometane: methanol = 20:1) to afford **13** (26 mg, 15%). ^{1}H NMR (400 MHz, DMSO-d_6): δ 8.61 (d, J = 5.2 Hz, 1H), 8.40 (d, J = 7.7 Hz, 1H), 8.21 (d, J = 9.0 Hz, 1H), 8.02–7.92 (m, 1H), 7.70 (dd, J = 9.1, 1.7 Hz, 1H), 7.50 (dd, J = 8.2, 1.8 Hz, 1H), 7.35–7.11 (m, 2H), 4.41–4.18 (m, 2H), 4.03 (s, 3H), 3.95 (d, J = 7.4 Hz, 2H), 3.85–3.74 (m, 1H), 3.23 (t, J = 11.7 Hz, 1H), 2.08–1.90 (m, 2H), 1.84–1.53 (m, 2H) ppm. ^{13}C NMR (101 MHz, DMSO-d_6): δ 161.20, 159.65, 149.49, 142.62, 140.61, 139.82 (d, J = 2.2 Hz), 137.10 (d, J = 6.3 Hz), 134.11, 125.53 (d, J = 2.8 Hz), 116.72, 114.84, 114.58, 109.71, 106.57, 75.36, 71.60, 70.05, 53.81, 46.32, 29.03, 27.28 ppm. Due to possible overlap or short relaxation time one carbon is missing. HRMS: *m/z*: calcd for $C_{22}H_{22}FIN_3O_4$ $[M+H]^+$: 538.0634 found: 538.0612. HPLC: t_R = 5.820 min (91% at 220 nm).

4.2. In vitro DNA gyrase and topoIV inhibitory activity

A Gyrase Supercoiling High Throughput Plate Assay Kit and a TopoIV Relaxation High Throughput Plate Assay Kit, available from Inspiralis (Norwich, UK), were used to determine the IC_{50} values of the compounds for *S. aureus* and *E. coli*.

Assays were performed on black streptavidin-coated 96-well microtiter plates (Thermo Scientific Pierce, Norwich, UK), and wells were first rehydrated with the supplied wash buffer (20 mM Tris-HCl (pH 7.6), 137 mM NaCl, 0.005% [w/v] BSA, and 0.05% [v/v] Tween-20). The biotinylated oligonucleotide diluted with the wash buffer was then immobilized in each well and the excess was removed with the wash buffer. 1.5 U of *S. aureus* or *E. coli* DNA gyrase (TopoIV) enzyme, together with 0.75 μg of relaxed (supercoiled) pNO1 plasmid as substrate, was incubated in the presence of 3 μl inhibitor solution in 10% DMSO and 0.008% Tween-20 at 37 °C for 30 min in a final reaction volume of 30 μl in assay buffer (*S. aureus* DNA gyrase: 40 mM HEPES. KOH (pH 7.6), 10 mM magnesium acetate, 10 mM DTT, 2 mM ATP, 500 mM potassium glutamate and 0.05 mg/mL albumin; *E. coli* DNA gyrase: 35 mM Tris.HCl (pH 7.5), 24 mM KCl, 4 mM $MgCl_2$, 2 mM DTT, 1.8 mM spermidine, 1 mM ATP, 6.5% (w/v) glycerol and 0.1 mg/mL albumin; *S. aureus* TopoIV: 50 mM Tris.HCl (7.5), 5 mM $MgCl_2$, 5 mM DTT, 1.5 mM ATP, 350 mM potassium glutamate, and 0.05 mg/mL albumin; *E. coli* TopoIV: 40 mM HEPES.KOH (pH 7.6), 100 mM potassium glutamate, 10 mM magnesium acetate, 10 mM DTT, 1 mM ATP, and 50 μg/mL albumin). The reaction was stopped by adding the TF buffer (50 mM NaOAc (pH 4.7), 50 mM NaCl, and 50 mM $MgCl_2$) to allow triplex formation (biotin oligonucleotide plasmid) for another 30 min. Finally, the unbound plasmid was washed off with the TF buffer and the Promega Diamond dye was added to the T10 buffer solution (10 mM Tris-HCl (pH 8.0), 1 mM EDTA). After 15 min, the solution was mixed and fluorescence was read using a Biotek Synergy H4 Hybrid microplate reader (excitation, 495 nm; emission, 537 nm). Two inhibitor concentrations of 100 and 1 μM were used for pre-screening. IC_{50} values were determined at seven inhibitor concentrations for those compounds that had less than 50% residual enzyme activity at the 100 μM concentration, whereas the other compounds were classified as inactive (IC_{50} > 100 μM). The inhibitor concentration at which the residual activity of the enzyme is 50% (IC_{50}) was calculated by a nonlinear regression-based fit of the inhibition curves using the log [inhibitor] versus slope of the reaction variables (four parameters) – symmetric equation, in GraphPad Prism 6.0 software (GraphPad Software, CA, USA). The IC_{50} value represents the average of two independent measurements. Gepotidacin was used as a positive control and showed an IC_{50} value for DNA gyrase of 0.374 μM and 0.244 μM for *S. aureus* and *E. coli,* and TopoIV of 8.30 μM and 0.049 μM for *S. aureus* and *E. coli*.

4.3. Human TopoIIα selectivity evaluation

A Human Topoisomerase II Alpha Relaxation High Throughput Plate Assay Kit, purchased from Inspiralis (Norwich, UK), was used to evaluate compounds' selectivity for the bacterial enzymes over the homologous human topoisomerase II. The assay was performed on black streptavidin-coated 96-well microtiter plates (Thermo Scientific Pierce). First, wells were rehydrated with the provided wash buffer (20 mM Tris-HCl (pH 7.6), 137 mM NaCl, 0.005% (*w/v*) BSA, 0.05% (*v/v*) Tween 20). Biotinylated oligonucleotide in wash buffer was immobilized in the wells and the excess oligonucleotide was washed off with wash buffer. 1.5 U of Human topoisomerase IIα enzyme was incubated together with 0.75 μg of supercoiled pNO1 plasmid as substrate in the presence of 3 μL inhibitor solution in 10% DMSO and 0.008% Tween 20 and 1 μL 30 mM ATP, at 37 °C for 30 min in a final reaction volume of 30 μL in buffer (50 mM Tris-HCl (pH 7.5), 125 mM NaCl, 10 mM $MgCl_2$, 5 mM DTT, and 100 μg/mL albumin). The reactions were stopped by adding the TF buffer (50 mM NaOAc (pH 4.7), 50 mM NaCl, and 50 mM $MgCl_2$) to allow triplex formation (biotin-oligonucleotide plasmid) for additional 30 min. Then, the unbound plasmid was washed off with TF buffer and the solution of Promega Diamond dye in T10 buffer (10 mM Tris-HCl (pH 8.0), 1 mM EDTA) was added. Ten minutes later, the solution was mixed and fluorescence was read using a Biotek Synergy H4 Hybrid microplate reader (excitation, 495 nm; emission, 537 nm). Screening was performed at an inhibitor concentration of 100 μM. Raw data were converted to mean values ± SD percent of residual enzyme activity determined by two independent measurements.

4.4. Antimicrobial evaluation

Minimum inhibitory concentrations (MICs) were determined by the broth microdilution method in 96-well plate format according to Clinical and Laboratory Standards Institute guidelines and European Committee on Antimicrobial Susceptibility Testing (EUCAST) recommendations. The bacterial suspension of the specific bacterial strain equivalent to the 0.5 McFarland turbidity standard was diluted with cation-adapted Mueller-Hinton broth with TES (Thermo Fisher Scientific) to obtain a final inoculum of 10^5 CFU/mL. The compounds dissolved in DMSO and the inoculum were mixed together and incubated at 35 °C for 20 h. After incubation, MIC values were determined by visual inspection, as the lowest dilution of compounds that did not show turbidity. MICs were determined against various bacterial strains. Tetracycline was used as a positive control on each assay plate and showed MIC values on *S. aureus* 0.25 μg/mL, *E. coli* 1 μg/mL, *E. coli* D22 1 μg/mL, *E. coli* N43 0.25 μg/mL, MRSAQA-12.1 > 4 μg/mL, MRSAQA-11.7 > 4 μg/mL.*P. aeruginosa* >4 μg/mL, *K. pneumoniae* >4 μg/mL, *A. baumanii* >4 μg/mL.

Time kill assay: Methicillin resistant *Staphylococcus aureus* (MRSA ATCC 43300) was grown in Brain Heart Infusion broth (BHI) overnight at 37 °C. The overnight culture was diluted to approximately 10^6 CFU/mL and then treated with the compound **12** or ciprofloxacin at MIC, 4 × MIC and 8 × MIC for 24 h. The untreated culture served as the control. Aliquots of the cultures were serially diluted in PBS and plated on BHI agar at the 0-, 2-, 4-, 6-, 8-, and 24-h time points. The CFU were calculated for each time point. Bactericidal concentrations were defined as those achieving a 99.9% (3log 10) reduction in CFU/mL compared to the starting inoculum. The experiment was performed in triplicate and repeated two times.

Post-antibiotic effect – PAE: PAE was determined by viable counting method according to McDonald et al. [40]. MRSA was grown in BHI overnight at 37 °C. The overnight culture was diluted to approximately 10^6 CFU/mL in BHI. Cultures were divided into 9 aliquots, three of which were treated with compound **12** or ciprofloxacin at 8 × MIC, and the remaining three served as untreated control. The cultures were incubated for 60 min and the bacteria harvested by centrifugation (5000 g, 5 min).

Bacteria were washed three times with BHI and finally, the cell pellets were resuspended in fresh BHI using volumes equivalent to the original culture volumes. The new cultures were then incubated at 37 °C. Samples were removed for viable counting before washing, immediately after washing (time 0) and at hourly intervals for 8 h. Samples were serially diluted in PBS, plated on BHI agar and the CFUs were calculated after incubation at 37 °C for 20 h. The duration (D) of the PAE was calculated according to D = T - C where T and C represent the time (h) required for the treated and untreated culture, respectively, to increase CFU by 10-fold (by 1 log 10 CFU/mL). The experiment was repeated two times.

Resistance development: The potential of MRSA to develop resistance to **12** was evaluated following a previously described procedure with some modifications [41]. Briefly, minimum inhibitory concentrations were determined as described above. Each day, bacteria from wells exposed to subinhibitory concentrations (½ × MIC) were harvested, adjusted to 10^5 CFU/mL and the inoculum was subjected to the next passage MIC testing. The procedure was repeated over a period of 14 days (14 passages). All concentrations were tested in triplicates, and ciprofloxacin was used for comparison. The experiment was repeated two times.

4.5. Metabolic activity assessment

HepG2 (ATCC, VA, USA) cell line were cultured in Dulbecco's Modified Eagle Medium (DMEM; Sigma-Aldrich, MO, USA) supplemented with 10% fetal bovine serum (Gibco, NY, USA), 2 mM L-glutamine, 100 U/mL penicillin and 100 μg/mL streptomycin (all from Sigma-Aldrich, MO, USA) in a humidified chamber at 37 °C and 5% CO_2. Cells were seeded into 96-well plates at a density of 8,000 cells per well and allowed to attach overnight. After 24 h, cells were treated with compound of interest (concentration range 1.25–100 μM) or corresponding vehicle as control. The metabolic activity was assessed after 72 h treatment using the CellTiter 96 Aqueous One Solution Cell Proliferation Assay (Promega, WI, USA). The absorbance was measured at 492 nm on an automated microplate reader Spark Multimode Microplate Reader (Tecan Group Ltd., Switzerland). The data were normalized and IC_{50} were calculated with GraphPad prism 9.3.1 software using a nonlinear regression. Results for compounds **11** and **13** are presented as IC_{50} values from two independent experiments, each conducted in duplicate. Results for compounds **5**–**10** and **12** are presented as %RA values of each compound from two independent experiments, each conducted in duplicate.

4.6. Cardiovascular hERG inhibition

The cardiovascular inhibition profile was completely outsourced. The hERG screening was performed at TCG Lifesciences Pvt. Ltd. in Kolkata, West Bengal, India, using a Fluorescence Polarization-based hERG binding assay (Invitrogen kit).

4.7. Fish embryo acute toxicity (FET) test

Experiments involving zebrafish were performed in accordance with the general rules stated in the OECD Guidelines for the Testing of Chemicals (OECD, 2013, Test No. 236) and in compliance with the European Directive 2010/63/EU and the ethical guidelines for the care and use of laboratory animals of the Institute of Molecular Genetics and Genetic Engineering, University of Belgrade. Wild type (AB) zebrafish were raised to adult stage in a temperature- and light-controlled facility at 28 °C and a standard 14:10-h light-dark photoperiod, and were fed with commercial dry food twice a day and *Artemia nauplii* daily. Embryos produced by pair-wise mating were collected, washed from debris and distributed into 24-well plates containing 1 mL of E3 medium (5 mM NaCl, 0.17 mM KCl, 0.33 mM $CaCl_2$ and 0.33 mM $MgSO_4$ in distilled water), and kept at 28 °C. For assessing acute (lethal) and developmental (teratogenic) toxicity, the embryos were treated with increasing concentrations of the tested compounds 6 h post fertilization (hpf). The highest tested dose was 25 μg/mL due to solubility and DMSO concentration limitations (0.25% max), except for **3** (primary stock 5 mg/mL, the highest tested dose was 12.5 μg/mL). DMSO (0.25%) was used as negative control, while doxorubicin (25 μg/mL) was used as positive control. Every 24 h, dead embryos were discarded and live embryos were photographed and inspected for signs of toxicity. Experiments were performed in triplicate, and 24 embryos were tested per concentration. At 120 hpf, embryos were photographed, anesthetized by the addition of 0.1% (w/v) tricaine solution (Sigma-Aldrich, St. Louis, MO), and killed by freezing at −20 °C.

4.8. In vivo efficacy

The studies were performed at Neosome Life Sciences, LLC. All procedures were performed according to NeoSome Institutional Animal Care and Use Committee (IACUC) and guidelines as well as OLAW standards prior to conduct.

4.8.1. Mouse tolerability studies

Compounds were test formulated in a 5% DMSO aqueous vehicle. All three compounds (**3**, **4**, and **12**) were initially dissolved in DMSO in a volume to achieve a final volume of 5% DMSO (tolerated by mice). Mice received a single dose of formulated test articles delivered through either intravenous (IV) or intraperitoneal (IP) injection. Dose concentrations and dose volumes were recorded.

4.8.2. Neutropenic mouse thigh infection efficacy

Test compounds were prepared fresh prior to the first dose. Test agents were formulated at 2 mg/mL in 5% DMSO, 25% hydroxypropyl-β-cyclodextrin, and 0.75% polysorbate 80. The compounds were vortexed and sonicated to dissolve. Test agents appeared cloudy but remained well suspended with little precipitation. Prior to dosing, dose solutions were vortexed. Test compounds were dosed via intraperitoneal injection at 2, 8, 14, and 20 h post infection. CD-1 female mice were utilized in a mouse infection model. MRSA BAA-1717 (TCH 1516) was prepared for infection from an overnight plate culture and adjusting to an OD of 0.1 at 625 nm. The adjusted bacterial suspension was further diluted to target an infecting inoculum of 1.0×10^5 CFU/mouse. The actual inoculum size was 2.0×10^5 CFU/mouse. Mice were inoculated with 100 μL of the prepared bacterial suspension via intramuscular injection into the right rear thigh. Beginning at 2 h post infection, mice were dosed with either test agents or positive control antibiotic. Mice receiving test agents were dosed via intraperitoneal injection at either 20 mL/kg or 40 mL/kg. Four animals were dosed per group. One group of four mice was euthanized at initiation of therapy (T = 2 h) and CFUs determined. All remaining mice were euthanized at 26 h post infection. At termination, thighs were aseptically excised, weighed, and homogenized to a uniform consistency in 2 mL of sterile saline. The homogenate was serially diluted and plated on bacterial growth media. The CFUs were enumerated after overnight incubation.

Declaration of competing interest

The authors declare that they have no known competing financial interests or personal relationships that could have appeared to influence the work reported in this paper.

Data availability

Data will be made available on request.

Acknowledgements

This work was supported by the Slovenian Research Agency (Grants P1-0017 and P1-0208, the young researcher's program numbers 39010 and 50503) and by Proof of Concept project NICKI of the National Institute of Chemistry, and University of Ljubljana Innovation Fund.

Appendix A. Supplementary data

Supplementary data to this article can be found online at https://doi.org/10.1016/j.ejmech.2023.115160.

References

[1] E. Tacconelli, E. Carrara, A. Savoldi, S. Harbarth, M. Mendelson, D.L. Monnet, C. Pulcini, G. Kahlmeter, J. Kluytmans, Y. Carmeli, M. Ouellette, K. Outterson, J. Patel, M. Cavaleri, E.M. Cox, C.R. Houchens, M.L. Grayson, P. Hansen, N. Singh, U. Theuretzbacher, N. Magrini, A.O. Aboderin, S.S. Al-Abri, N. Awang Jalil, N. Benzonana, S. Bhattacharya, A.J. Brink, F.R. Burkert, O. Cars, G. Cornaglia, O. J. Dyar, A.W. Friedrich, A.C. Gales, S. Gandra, C.G. Giske, D.A. Goff, H. Goossens, T. Gottlieb, M. Guzman Blanco, W. Hryniewicz, D. Kattula, T. Jinks, S.S. Kanj, L. Kerr, M.P. Kieny, Y.S. Kim, R.S. Kozlov, J. Labarca, R. Laxminarayan, K. Leder, L. Leibovici, G. Levy-Hara, J. Littman, S. Malhotra-Kumar, V. Manchanda, L. Moja, B. Ndoye, A. Pan, D.L. Paterson, M. Paul, H. Qiu, P. Ramon-Pardo, J. Rodríguez-Baño, M. Sanguinetti, S. Sengupta, M. Sharland, M. Si-Mehand, L.L. Silver, W. Song, M. Steinbakk, J. Thomsen, G.E. Thwaites, J.W. van der Meer, N. Van Kinh, S. Vega, M.V. Villegas, A. Wechsler-Fördös, H.F.L. Wertheim, E. Wesangula, N. Woodford, F.O. Yilmaz, A. Zorzet, Discovery, research, and development of new antibiotics: the WHO priority list of antibiotic-resistant bacteria and tuberculosis, Lancet Infect. Dis. 18 (2018) 318–327.

[2] U.S. Department, Of Health and Human Services, Centers for Disease Control and Prevention., 2019. https://www.cdc.gov/drugresistance/biggest_threats.html. (Accessed 24 May 2022). accessed.

[3] G.H. Dayan, N. Mohamed, I.L. Scully, D. Cooper, E. Begier, J. Eiden, K.U. Jansen, A. Gurtman, A.S. Anderson, Staphylococcus aureus: the current state of disease, pathophysiology and strategies for prevention, Expert Rev. Vaccines 15 (2016) 1373–1392, https://doi.org/10.1080/14760584.2016.1179583.

[4] N.G. Bush, K. Evans-Roberts, A. Maxwell, DNA topoisomerases, EcoSal Plus 6 (2015) 1–34.

[5] K. Drlica, M. Malik, Fluoroquinolones: action and resistance, Curr. Top. Med. Chem. 3 (2003) 249–282.

[6] LiverTox, Clinical and Research Information on Drug-Induced Liver Injury, Fluoroquinolones., 2020. https://www.ncbi.nlm.nih.gov/books/NBK547840/?report=classic.

[7] Novel Drug Approvals for 2017, n.d. https://www.fda.gov/drugs/new-drugs-fda-cders-new-molecular-entities-and-new-therapeutic-biological-products/novel-drug-approvals-2017. (Accessed 24 May 2022).

[8] L.J. Scott, Delafloxacin : a review in acute bacterial skin and skin structure infections, Drugs 80 (2020) 1247–1258.

[9] S.C.J. Jorgensen, N.J. Mercuro, S.L. Davis, Delafloxacin : place in therapy and review of microbiologic , clinical and pharmacologic properties, Infect. Dis. Ther. 7 (2018) 197–217.

[10] Y.-C. Tse-Dinh, Targeting bacterial topoisomerases - how to counter mechanisms of resistance, Future Med. Chem. 8 (2016) 1085–1100.

[11] A.A. Miller, G.L. Bundy, J.E. Mott, J.E. Skepner, T.P. Boyle, D.W. Harris, A. E. Hromockyj, K.R. Marotti, G.E. Zurenko, J.B. Munzner, M.T. Sweeney, G. F. Bammert, J.C. Hamel, C.W. Ford, W.Z. Zhong, D.R. Graber, G.E. Martin, F. Han, L.A. Dolak, E.P. Seest, J.C. Ruble, G.M. Kamilar, J.R. Palmer, L.S. Banitt, A.R. Hurd, M.R. Barbachyn, Discovery and characterization of QPT-1, the progenitor of a new class of bacterial topoisomerase inhibitors, Antimicrob. Agents Chemother. 52 (2008) 2806–2812.

[12] P.A. Bradford, A.A. Miller, J. O'Donnell, J.P. Mueller, Zoliflodacin: an oral spiropyrimidinetrione antibiotic for the treatment of Neisseria gonorrheae, including multi-drug-resistant isolates, ACS Infect. Dis. 6 (2020) 1332–1345.

[13] J.J.M. Wiener, L. Gomez, H. Venkatesan, A. Santillán, B.D. Allison, K.L. Schwarz, S. Shinde, L. Tang, M.D. Hack, B.J. Morrow, S.T. Motley, R.M. Goldschmidt, K. J. Shaw, T.K. Jones, C.A. Grice, Tetrahydroindazole inhibitors of bacterial type II topoisomerases. Part 2: SAR development and potency against multidrug-resistant strains, Bioorg. Med. Chem. Lett 17 (2007) 2718–2722.

[14] M.T. Black, T. Stachyra, D. Platel, A.M. Girard, M. Claudon, J.M. Bruneau, C. Miossec, Mechanism of action of the antibiotic NXL101, a novel nonfluoroquinolone inhibitor of bacterial type II topoisomerases, Antimicrob. Agents Chemother. 52 (2008) 3339–3349.

[15] B.D. Bax, P.F. Chan, D.S. Eggleston, A. Fosberry, D.R. Gentry, F. Gorrec, I. Giordano, M.M. Hann, A. Hennessy, M. Hibbs, J. Huang, E. Jones, J. Jones, K. K. Brown, C.J. Lewis, E.W. May, M.R. Saunders, O. Singh, C.E. Spitzfaden, C. Shen, A. Shillings, A.J. Theobald, A. Wohlkonig, N.D. Pearson, M.N. Gwynn, Type IIA topoisomerase inhibition by a new class of antibacterial agents, Nature 466 (2010) 935–940.

[16] A. Kolarič, M. Anderluh, N. Minovski, Two decades of successful SAR-grounded stories of the novel bacterial topoisomerase inhibitors (NBTIs), J. Med. Chem. 63 (2020) 5664–5674.

[17] A. Kolarič, T. Germe, M. Hrast, C.E.M. Stevenson, D.M. Lawson, N.P. Burton, J. Vörös, A. Maxwell, N. Minovski, M. Anderluh, Potent DNA gyrase inhibitors bind asymmetrically to their target using symmetrical bifurcated halogen bonds, Nat. Commun. 12 (2021) 1–13.

[18] E.G. Gibson, B. Bax, P.F. Chan, N. Osheroff, Mechanistic and structural basis for the actions of the antibacterial gepotidacin against staphylococcus aureus gyrase, ACS Infect. Dis. 5 (2019) 570–581.

[19] M. Kokot, M. Anderluh, M. Hrast, N. Minovski, The structural features of novel bacterial topoisomerase inhibitors that define their activity on topoisomerase IV, J. Med. Chem. 65 (2022) 6431–6440.

[20] N.E. Scangarella-Oman, M. Hossain, P.B. Dixon, K. Ingraham, S. Min, C.A. Tiffany, C.R. Perry, A. Raychaudhuri, E.F. Dumont, J. Huang, E.W. 3rd Hook, L.A. Miller, Microbiological analysis from a phase 2 randomized study in adults evaluating single oral doses of gepotidacin in the treatment of uncomplicated urogenital gonorrhea caused by Neisseria gonorrhoeae, Antimicrob. Agents Chemother. 62 (2018) e01221-18.

[21] A Study Evaluating Efficacy and Safety of Gepotidacin Compared with Ceftriaxone Plus Azithromycin in the Treatment of Uncomplicated Urogenital Gonorrhea, 2019. https://clinicaltrials.gov/ct2/show/NCT04010539?cond=gepotidacin&draw=2&rank=1. (Accessed 6 September 2022). accessed.

[22] N.E. Scangarella-Oman, M. Hossain, J.L. Hoover, C.R. Perry, C. Tiffany, A. Barth, E. F. Dumont, Dose selection for phase III clinical evaluation of gepotidacin (GSK2140944) in the treatment of uncomplicated urinary tract infections, Antimicrob. Agents Chemother. 66 (2022), e0149221.

[23] A. Kolarič, N. Minovski, Novel bacterial topoisomerase inhibitors: challenges and perspectives in reducing hERG toxicity, Future Med. Chem. 10 (2018) 2241–2244.

[24] F. Reck, R. Alm, P. Brassil, J. Newman, B. DeJonge, C.J. Eyermann, G. Breault, J. Breen, J. Comita-prevoir, M. Cronin, H. Davis, D.E. Ehmann, V. Galullo, B. Geng, T. Grebe, M. Morningstar, P. Walker, B. Hayter, S. Fisher, Novel N-linked aminopiperidine inhibitors of bacterial topoisomerase type II: broad-spectrum antibacterial agents with reduced hERG activity, J. Med. Chem. 54 (2011) 7834–7847.

[25] L. Li, A.A. Okumu, S. Nolan, A. English, S. Vibhute, Y. Lu, K. Hervert-Thomas, J. T. Seffernick, L. Azap, S.L. Cole, D. Shinabarger, L.M. Koeth, S. Lindert, J. C. Yalowich, D.J. Wozniak, M.J. Mitton-Fry, 1,3-Dioxane-Linked bacterial topoisomerase inhibitors with enhanced antibacterial activity and reduced hERG inhibition, ACS Infect. Dis. 5 (2019) 1115–1128.

[26] A. Garrido, A. Lepailleur, S.M. Mignani, P. Dallemagne, C. Rochais, hERG toxicity assessment: useful guidelines for drug design, Eur. J. Med. Chem. 195 (2020), 112290.

[27] B.D. Bax, G. Murshudov, A. Maxwell, T. Germe, DNA topoisomerase inhibitors: trapping a DNA-cleaving machine in motion, J. Mol. Biol. 431 (2019) 3427–3449.

[28] M. Kokot, M. Weiss, I. Zdovc, M. Anderluh, M. Hrast, N. Minovski, Diminishing hERG cardiotoxic potential of aminopiperidine-naphthyridine linked NBTI antibacterials by structural and physico-chemical optimizations, Bioorg. Chem. 128 (2022), 106087.

[29] Y. Lu, J.L. Papa, S. Nolan, A. English, J.T. Seffernick, N. Shkolnikov, J. Powell, S. Lindert, D.J. Wozniak, J. Yalowich, M.J. Mitton-Fry, Dioxane-linked amide derivatives as novel bacterial topoisomerase inhibitors against gram-positive Staphylococcus aureus, ACS Med. Chem. Lett. 11 (2020) 2446–2454.

[30] Y. Lu, C.A. Mann, S. Nolan, J.A. Collins, E. Parker, J. Papa, S. Vibhute, S. Jahanbakhsh, M. Thwaites, D. Hufnagel, M.H. Hazbón, J. Moreno, T.T. Stedman, T. Wittum, D.J. Wozniak, N. Osheroff, J.C. Yalowich, M.J. Mitton-Fry, 1,3-Dioxane-Linked novel bacterial topoisomerase inhibitors: expanding structural diversity and the antibacterial spectrum, ACS Med. Chem. Lett. 13 (2022) 955–963, https://doi.org/10.1021/acsmedchemlett.2c00111.

[31] C. Zumbrunn, A short history of topoisomerases at actelion pharmaceuticals, Chimia 76 (2022) 647, https://doi.org/10.2533/chimia.2022.647.

[32] M. Kokot, M. Weiss, I. Zdovc, M. Hrast, M. Anderluh, N. Minovski, Structurally optimized potent dual-targeting NBTI antibacterials with an enhanced bifurcated halogen-bonding propensity, ACS Med. Chem. Lett. 12 (2021) 1478–1485.

[33] A. Kolarič, M. Kokot, M. Hrast, M. Weiss, I. Zdovc, J. Trontelj, S. Žakelj, M. Anderluh, N. Minovski, A fine-tuned lipophilicity/hydrophilicity ratio governs antibacterial potency and selectivity of bifurcated halogen, Antibiotics 10 (2021) 862.

[34] M. Hossain, M. Zhou, C. Tiffany, E. Dumont, B. Darpo, A phase I, randomized, double-blinded, placebo-and moxifloxacin-controlled, four-period crossover study to evaluate the effect of gepotidacin on cardiac conduction as assessed by 12-lead electrocardiogram in healthy volunteers, Antimicrob, Agents Chemother 61 (2017) 1–9.

[35] M.F. Richter, B.S. Drown, A.P. Riley, A. Garcia, T. Shirai, R.L. Svec, P. J. Hergenrother, Predictive compound accumulation rules yield a broad-spectrum antibiotic, Nature 545 (2017) 299–304, https://doi.org/10.1038/nature22308.

[36] S. Cassar, I. Adatto, J.L. Freeman, J.T. Gamse, C. Lawrence, A. Muriana, R. T. Peterson, S. Van Cruchten, L.I. Zon, N. Chicago, U. States, R. Biology, U. States, W. Lafayette, U. States, S. Evaluation, B. Squibb, N. Brunswick, U. States, R. Program, S.L. City, U. States, C. Program, D. Farber, H.S. Cell, S. Cell, U. States, Use of zebrafish in drug discovery toxicology, Chem. Res. Toxicol. 33 (2020) 95–118.

[37] U. Langheinrich, G. Vacun, T. Wagner, Zebrafish embryos express an orthologue of HERG and are sensitive toward a range of QT-prolonging drugs inducing severe arrhythmia, Toxicol. Appl. Pharmacol. 193 (2003) 370–382.
[38] A. Al Shoyaib, S.R. Archie, V.T. Karamyan, Intraperitoneal route of drug administration: should it Be used in experimental animal studies? Pharm. Res. (N. Y.) 37 (2020) https://doi.org/10.1007/s11095-019-2745-x.
[39] N. D'Atanasio, A.C. de Joannon, L. Di Sante, G. Mangano, R. Ombrato, M. Vitiello, C. Bartella, G. Magarò, F. Prati, C. Milanese, C. Vignaroli, F.P. Di Giorgio, S. Tongiani, Antibacterial activity of novel dual bacterial DNA type II topoisomerase inhibitors, PLoS One 15 (2020) 1–21.
[40] P.J. McDonald, W.A. Craig, C.M. Kunin, Persistent effect of antibiotics on Staphylococcus aureus after exposure for limited periods of time, J. Infect. Dis. 135 (1977) 217–223, https://doi.org/10.1093/infdis/135.2.217.
[41] Z. Li, X. Xu, L. Meng, Q. Zhang, L. Cao, W. Li, Y. Wu, Z. Cao, Hp1404, a new antimicrobial peptide from the scorpion Heterometrus petersii, PLoS One 9 (2014), e97539, https://doi.org/10.1371/journal.pone.0097539.